Macromolecular Chemistry and Physics

Macromolecular Chemistry and Physics
www.mcp-journal.de

RESEARCH ARTICLE OPEN ACCESS

Synthesis of Non-Isocyanate Poly(Sulfide Urethane) Adhesives by Thermally Initiated Thiol-Ene Polymerization

Nichollas G. Jaques[1,2] | Audrey Llevot[1] | Thomas Vidil[1] | Étienne Grau[1] | Olaf Hartman[3] | Henri Cramail[1] | Michael A. R. Meier[2]

[1]Univ. Bordeaux, CNRS, Bordeaux INP, LCPO UMR5629, 16 avenue Pey-Berland, Pessac, France | [2]Institute of Organic Chemistry (IOC) & Institute of Biological and Chemical Systems – Functional Molecular Systems (IBCS-FMS), Karlsruhe Institute of Technology, Karlsruhe, Germany | [3]Henkel AG & Co. KGaA, Düsseldorf, Germany

Correspondence: Henri Cramail (cramail@enscbp.fr) | Michael A. R. Meier (m.a.r.meier@kit.edu)

Received: 16 October 2025 | **Revised:** 23 December 2025 | **Accepted:** 12 January 2026

Keywords: adhesive transurethanization | thermal-initiation non-isocyanate polyurethane (NIPU) | thiol-Ene

ABSTRACT

Three synthetic routes, thermally initiated thiol-ene polyaddition, isocyanate-based polyaddition, and transurethanization, were compared for the synthesis of non-isocyanate poly(urethane)s (NIPUs). Relatively high molecular weight polymers (M_n up to 19 kg×mol^{-1}) were successfully achieved via thiol-ene coupling using α,ω-diene-functionalized carbamates and aliphatic dithiols as monomers under solvent-free conditions and dicumyl peroxide as a thermal initiator at a [SH]/[Ene] ratio of 1.05. Compared to conventional isocyanate and transurethanization methods, the thiol-ene approach demonstrated slightly higher molar mass and reduced formation of urea and carbonate byproducts, independent of the formulation prepared. Thermal and mechanical characterization revealed that NIPUs, especially the ones prepared via thiol-ene, exhibited thermal transitions, tensile strength, and elongation at break comparable to or superior to those of their isocyanate-based counterparts. Adhesive performance was further enhanced through a thermally activated thiol-ene reactive bonding strategy, where in situ polymerization at the substrate interface led to a fourfold increase in lap shear strength (8 MPa) compared to a thermoplastic hot-melt application (2 MPa). These findings highlight that thermally initiated thiol-ene polyaddition is promising for the synthesis of high-performance, isocyanate-free polyurethane materials with potential applications in coatings, adhesives, and thermoplastics.

1 Introduction

Sulfur-containing polyurethanes, such as poly(thiourethane)s, poly(thiourethane urethane)s, and poly(sulfide urethane)s, represent a versatile class of functional polymers with unique physicochemical properties [1, 2]. These include high refractive index, strong adhesion, tunable mechanical properties, chemical resistance, and biocompatibility, i.e. characteristics attributed to the capacity of sulfur to form weak hydrogen bonding, and the longer C—S bond length compared to C—C and C—O bonds [1–4]. Such features have enabled applications of these polymers in optics, electronics, coatings, adhesives, and biomedical materials [3].

Like conventional polyurethanes, sulfur-containing analogues are typically synthesized from isocyanates. For instance, poly(thiourethane)s result from the polyaddition of thiols with isocyanates, while poly(sulfide urethane)s are formed via polyaddition of isocyanates with sulfide-containing diols or via thiol-ene coupling [1, 3, 5]. However, isocyanates are toxic and moisture-sensitive. These molecules have thus been increasingly restricted by regulatory frameworks such as REACH [6]. In

response, non-isocyanate polyurethanes (NIPUs) have gained attention as safer and more sustainable alternatives [7, 8].

Several strategies have been explored for synthesizing sulfur-containing NIPUs. These include the aminolysis of dithiocarbonates to yield polythiourethanes [9, 10], the thiol-induced decarboxylation of cyclic carbonates in the presence of amines [11, 12], or the use of sulfide- or disulfide-functionalized cyclic carbonates and/or amines [13, 14]. These approaches have been mainly applied to produce thermoset foams, adhesives, and vitrimeric materials [9, 11]. Nonetheless, these methods often suffer from low reactivity, limited conversion, and side-product formation [9, 11]. Moreover, the resulting chemical structure diverges from those prepared via isocyanate-based routes, leading to distinct thermal behavior and limiting their utility in thermoplastic applications [14].

An alternative route that has recently emerged involves thiol-ene coupling, a radical-mediated reaction between thiols and C=C double bonds [5, 15–17]. This approach offers efficiency, high atom economy, mild reaction conditions, and controlled byproduct formation, features that align with green chemistry principles [5]. While thiol-ene chemistry has been applied to synthesize biosourced building blocks for NIPUs such as diamines [14, 18] and cyclic carbonates [19, 20], its potential to create thermoplastic poly(sulfide urethane)s with tunable properties has not been fully explored yet [5, 16, 21].

Initially, most of the current studies were dedicated to the synthesis of monomers with carbamate and ene motifs that were subsequently polymerized via thiol-ene coupling. Reported strategies include the reaction of cysteamine with allyl chloroformate [17], the reaction of *N*-substituted carbamic acid esters in the presence of ω-halogenated alkenes [16], the aminolysis of cyclic carbonates with allyl or fatty-acid-derived amines [15], and the Lossen rearrangement of hydroxamic acids in the presence of allyl alcohol [5]. While some of these approaches utilize toxic halogenated reagents, greener alternatives still suffer from incomplete conversion and side-product formation.

A more sustainable and efficient route was demonstrated by Burel et al. in 2016 [22]. The authors demonstrated the synthesis of α,ω-diene-functionalized polyurethanes and polyureas via transurethanization with oleic acid derivatives, with minimal side reactions [22]. Alternatively, Xie et al. [16]. investigated the ADMET and thiol-ene polymerization of α,ω-diene carbamates synthesized from *N*-substituted carbamic acid esters and ω-halogenated alkenes. The authors reported that the resulting non-isocyanate poly(sulfide urethane)s, prepared via photoinitiated thiol-ene coupling, achieved limited molar masses (M_n up to 11 kg×mol^{-1}) even after extended reaction times (~24 h).

Although the thiol-ene approach has been applied to prepare thermoplastic poly(sulfide urethane)s, a direct comparison of their properties with sulfur-containing polyurethanes synthesized via traditional isocyanate-based or transurethanization methods is lacking. Importantly, the thiol-ene route avoids the formation of urea byproducts, commonly observed during isocyanate hydrolysis or carbamate metathesis [23]. This absence of urea moieties could have a significant impact on the final thermal and mechanical properties of the polymers.

In this work, α,ω-diene carbamates were synthesized via transurethanization of dimethyl carbamates with 10-undecen-1-ol, derived from castor oil. The latter were then polymerized through thiol-ene coupling under thermal-initiated conditions. In parallel, sulfide-containing diols were obtained by thiol-ene addition of 10-undecen-1-ol with dithiols and subsequently polymerized via either transurethanization or isocyanate-based polyaddition. The effect of the synthetic route on the obtained molecular weights and the resulting chemical structure was evaluated in terms of side-product formation, hydrogen bonding, and morphology. Additionally, the influence of polymer structure on thermal, mechanical, and adhesive properties was assessed. To the best of our knowledge, this is the first direct comparison of synthetic strategies toward poly(sulfide urethane)s, offering new insights into the design of greener, thermoplastic, sulfur-rich polyurethanes.

2 Materials and Methods

2.1 Materials

Dicumyl peroxide (**DCP**, 98%), 1,8-dimercapto-3,6-dioxaoctane (**9**, 95%), and isophorone diisocyanate (**13**, 98%) were purchased from Sigma–Aldrich. Potassium *tert*-butoxide (KO^{t}Bu, 97%), 1,10-decanedithiol (**10**, 95%,) and 1,5,7-triazabicyclo[4.4.0]dec-5-ene (TBD, 98%) were purchased from TCI. 1,6-Hexamethylene diisocyanate (**14**, 98%) and 1,6-hexanediamine (**2**, 99.5%) were acquired from Fischer Scientific. Dimethyl carbonate (**1**, 99%) and isophorone diamine (**3**, 99%) were purchased from Acros Organics. 10-Undecen-1-ol (**6**, 99%) was acquired from ABCR. $CDCl_3$ was obtained from VWR and deuterated dimethyl sulfoxide (DMSO-d_6, 99.5%) was obtained from Eurisotop.

2.2 Methods

2.2.1 Synthesis

2.2.1.1 Synthesis of Bismethyl Carbamates 4 and 5. Bismethyl carbamates were synthesized by the methoxycarbonylation of different diamines (1,6-hexanediamine (**2**) and isophorone diamine (**3**)) (1 equiv. mol, 172 mmol) in a 500 mL Schlenk flask with an excess of dimethyl carbonate (**1**, 10 equiv., 1721 mmol) in the presence of TBD as a catalyst (0.05 equiv., 8.6 mmol), as shown in Scheme 1. The reaction was performed with magnetic stirring under a static nitrogen atmosphere at 80°C for 24 h. Then, the excess of dimethyl carbonate and methanol generated during the methoxycarbonylation of diamine were removed under vacuum at 65°C.

Further purification of crystalline dimethyl hexane-1,6-diyldicarbamate (**4**) was performed via recrystallization from cold methanol using an ice bath. The product was filtered and dried in a vacuum oven at 65°C for 12 h. The product was obtained as a white crystalline powder with a yield of 85%.

^{1}H NMR (400 MHz, DMSO-d_6): δ (ppm) = 7.06 (s, 2H), 3.50 (s, 6H), 2.93 (s, 4H), 1.36 (s, 4H), 1.23 (s, 4H).

^{13}C NMR (400 MHz, DMSO-d_6): δ (ppm) = 157.11, 51.54, 29.88, 29.45, 29.20, 26.69.

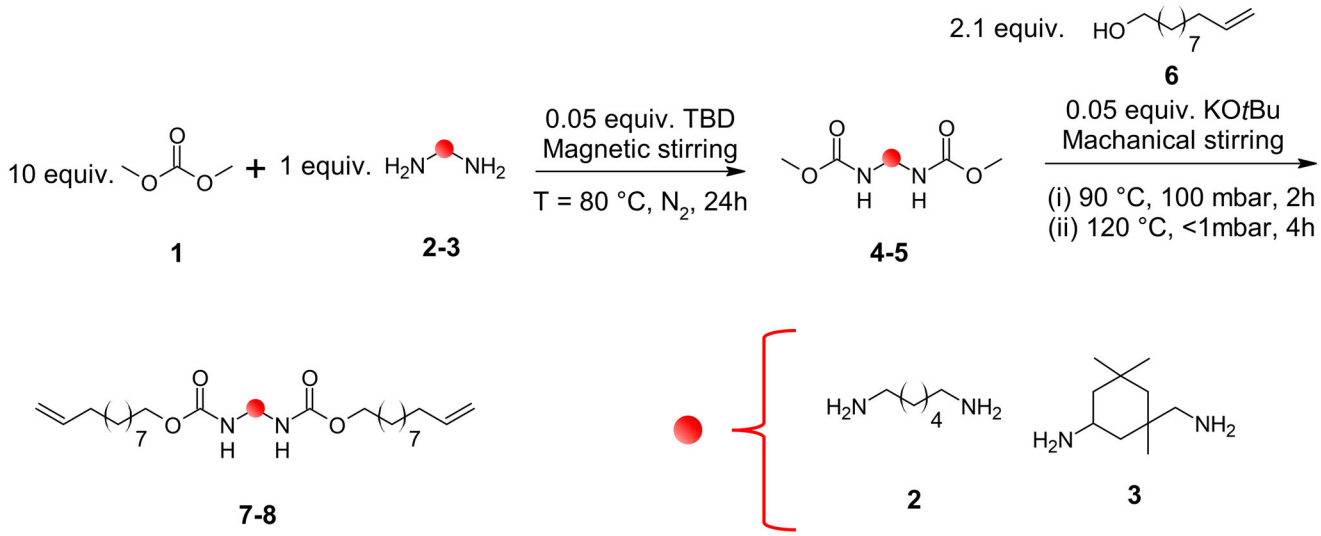

SCHEME 1 | Synthesis of dimethyl carbamates (**1**) by methoxycarbonylation of amines (**2** or **3**), followed by the synthesis of α,ω-diene carbamates via transurethanization in the presence of 10-undecen-1-ol.

Methyl ((5-((methoxycarbonyl)amino)-1,3,3-trimethylcyclohexyl) methyl)carbamate (**5**) was purified as follows: the product was solubilized in dichloromethane (DCM) and washed with 5%.wt HCl solution, followed by washing with brine to remove the catalyst and remaining non-reacted diamine. Finally, DCM was removed under vacuum at 45°C for 12 h. **5** was obtained as a transparent solid product with a yield of 90%.

^{1}H NMR (400 MHz, DMSO-d_6): δ = 7.11-7.06 (t, 2H), 3.56 (s, 1H), 3.51-3.49 (s, 6H), 3.10-2.77 (m, 2H), 1.66-0.77 (16H).

^{13}C NMR (400 MHz, DMSO-d_6): δ (ppm) = 157.33, 157.18, 155.88, 155.8, 54.90, 54.24, 51.20, 50.98, 47.55, 46.86, 46.59, 45.81, 45.48, 43.92, 41.65, 41.28, 36.26, 35.69, 34.99, 31.40, 29.87, 27.50, 26.99, 23.19.

2.2.1.2 Synthesis of Double Bond Terminated Carbamates 7 and 8. The synthesis of double bond terminated carbamates **7** and **8** was performed inspired by previous investigations [22]. Bismethyl carbamates (**4** or **5**, 1 equiv. 52.4 mmol) and 10-undecen-1-ol (**6**, 3 equiv, 157.2 mmol), in the presence of potassium *tert*-butoxide (KO^{t}Bu, 0.1 equiv., 5.2 mmol), were added to a 100 mL round-bottom Schlenk flask equipped with mechanical stirring and vacuum inlet. The reaction was performed initially at 90°C under a pressure of 50 mbar for 2 h. After that, the temperature was progressively increased to 120°C and the pressure decreased (< 1 mbar) for an additional 2 h to remove any excess of methanol and unreacted 1-undecen-10-ol.

The aliphatic di(undec-10-en-1-yl) hexane-1,6-diyldicarbamate (**7**) was purified by recrystallization using hot DMSO. The product was then washed with methanol, filtered, and dried in a vacuum oven at 65°C for 12 h. It was obtained as a white crystalline powder with a yield of 85%.

^{1}H NMR (400 MHz, $CDCl_3$): δ = 5.80 (ddt, J = 16.9, 10.2, 6.7 Hz, 2H), 5.06 – 4.86 (m, 4H), 4.65 (s, 2H), 4.02 (t, J = 6.8 Hz, 4H), 3.15 (q, J = 6.8 Hz, 4H), 2.13 – 1.92 (m, 4H), 1.58 (q, J = 7.0 Hz, 4H), 1.48 (p, J = 6.9 Hz, 4H), 1.41 – 1.21 (m, 28H).

^{13}C NMR (400 MHz, v): δ (ppm) = 156.98, 139.37, 114.27, 65.08, 40.91, 33.95, 29.25, 26.43, 26.02.

Undec-10-en-1-yl((1,3,3-trimethyl-5-(((undec-10-en-1-yloxy)carbonyl)amino) cyclohexyl) methyl)carbamate (**8**) was isolated by column chromatography using hexane:ethyl acetate = 9:1 as eluent. Then, the carbamate was further purified in a Kugelrohr distillation system at 135°C for 6 h. The product was obtained as a yellow viscous liquid with a yield of 63%.

^{1}H NMR (400 MHz, $CDCl_3$): δ (pm) = 5.76 (ddt, J = 16.9, 10.2, 6.7 Hz, 2H), 4.98–4.85 (m, 5H), 4.85–4.67 (m, 1H), 4.56 (d, J = 8.0 Hz, 1H), 3.99 (p, J = 9.5, 7.9 Hz, 4H), 3.71 (dt, J = 45.2, 12.9 Hz, 1H), 3.33–2.77 (m, 2H), 2.08 (s, 1H), 1.99 (q, J = 7.0 Hz, 5H), 1.88–0.66 (m, 51H).

^{13}C NMR (400 MHz, $CDCl_3$): δ (ppm) = 157.23, 156.07, 139.13, 114.18, 65.05, 54.90, 47.15, 46.44, 44.54, 41.94, 36.43, 35.09, 33.83, 31.87, 27.65, 25.90, 23.24.

2.2.1.3 Synthesis of Thio-Ether Containing Diols 11 and 12. Sulphur-containing diols were synthesized by thiol-ene reaction, based on an adapted methodology previously proposed [24]. 1,8-Dimercapto-3,6-dioxaoctane (**9**, 1 equiv., 41.9 mmol) or 1,10-decanedithiol (**10**, 1 equiv., 41.9 mmol) and 10-undecen-1-ol (**6**, 2.1 equiv., 88.1 mmol) were added to a 100 mL round-bottom Schlenk flask with a nitrogen inlet in the presence of 2,2-dimethoxy-2-phenylacetophenone as photoinitiator (DMPA, 0.02 equiv., 0.88 mmol). The reaction medium was exposed to an ultraviolet light source with a wavelength of 365 nm for 6 h (Scheme S2).

The further purification of crystalline 15,18-dioxa-12,21-dithiadotriacontane-1,32-diol (**11**) and 11,11'-(decane-1,10-diylbis(sulfanediyl))bis(undecan-1-ol) (**12**) was performed via recrystallization from cold ethyl acetate using an ice bath. The product was filtered and dried in a vacuum oven at 65°C for 12 h. The products were obtained as white crystalline powder with a yield of 72% and 67%, respectively.

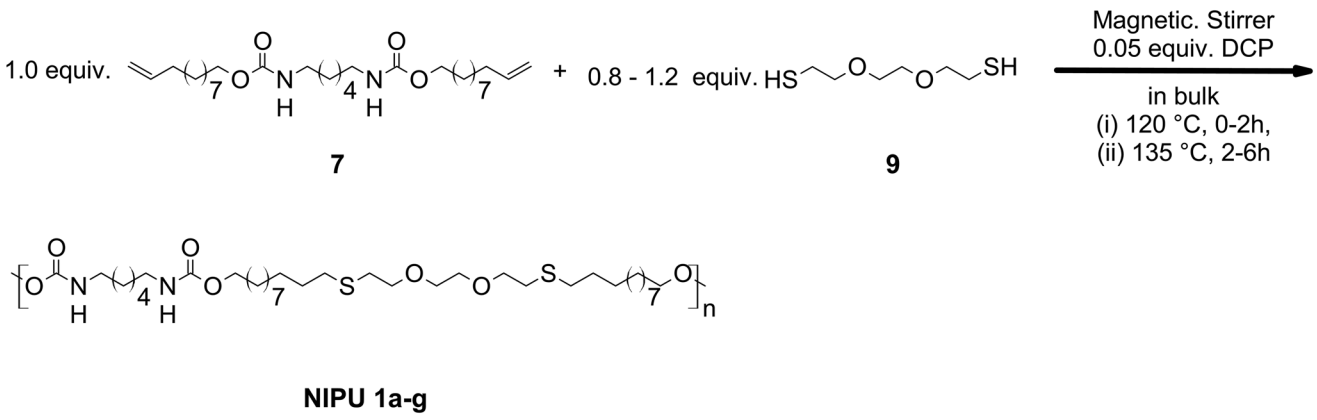

SCHEME 2 | Polymerization leading to poly(sulfide urethane)s **NIPU 1a-g** via thermally activated thiol-ene of α,ω-diene carbamate (**7**) in the presence of 1,8-dimercapto-3,6-dioxaoctane (**9**).

Diol **11**:

^{1}H NMR (400 MHz, $CDCl_3$): δ (ppm) = 3.68–3.59 (m, 12H), 2.71 (t, J = 7.1 Hz, 4H), 2.61–2.48 (m, 4H), 1.63–1.51 (m, 10H), 1.40–1.21 (m, 30H).

^{13}C NMR (400 MHz, $CDCl_3$): δ (pmm) = 71.19, 70.42, 63.18, 32.92, 32.72, 31.48, 29.92, 29.69, 29.61, 29.53, 29.35, 25.85.

Diol **12**:

^{1}H NMR (400 MHz, $CDCl_3$): δ (ppm) = 3.64 (t, J = 6.3 Hz, 4H), 2.54–2.46 (m, 8H), 1.56 (q, J = 8.1, 7.5 Hz, 16H), 1.32 (d, J = 34.7 Hz, 46H).

^{13}C NMR (400 MHz, DMSO-d_6): δ (ppm) = 157.23, 156.07, 139.13, 114.18, 65.05, 54.90, 47.15, 46.44, 44.54, 41.94, 36.43, 35.09, 33.83, 31.87, 27.65, 25.90, 23.24.

2.2.1.4 Synthesis of NIPU by Thermally Initiated Thiol-Ene. Thermally initiated thiol-ene reactions of di(undec-10-en-1-yl) hexane-1,6-diyldicarbamate (**7**) and 1,8-dimercapto-3,6-dioxaoctane (**9**) using dicumyl peroxide (**DCP**, 0.05 equiv.) as a radical initiator were carried out in a 50 mL round-bottom Schlenk flask attached to a mechanical stirrer and a nitrogen inlet following the indicated temperature program: (i) 120°C for 2 h, (ii) 135°C for 4 h (**NIPU 1**). The reaction was assessed using different thiol to ene molar ratios ([SH]/[Ene]), that varied from 0.8 to 1.2 equiv. mol, as depicted in Scheme 2. **NIPU 2a**, prepared by the polyaddition of **8** and 1,10-decanedithiol (**10**), and **NIPU 3a**, synthesized by the polyaddition of **7** and **10**, were prepared using a [SH]/[Ene] = 1.05. The polymers were characterized without further purification.

2.2.1.5 Synthesis of the NIPUs by Transurethanization. NIPUs were synthesized under optimized transurethanization conditions, as suggested in our previous work [23]. The compounds were prepared using 0.05 equiv. of KO^{t}Bu relative to the carbamate content, with a hydroxyl and carbamate molar ratio ([OH]/[Carb.]) of 0.90. The compositions were prepared using the bismethyl carbamates (**4** or **5**) with diol (**12**) as indicated in Scheme 3. The selected carbamates and diols were added to a 50 mL round-bottom Schlenk flask attached to a vacuum line following the indicated condition: (i) 120°C for 2 h under a pressure of 100 mbar. (ii) 135°C for 4 h under a pressure of < 1 mbar.

2.2.1.6 Synthesis of Reference Polyurethane. Reference polyurethanes **PU 1** and **PU 2** were prepared using a similar temperature protocol proposed for the transurethanization. The reaction was mechanically stirred in a 50 mL round-bottom Schlenk flask with continuous nitrogen flow. First, isophorone diisocyanate (**13,** 1 equiv.) (**PU 1**) or hexamethylene diisocyanate (**14**, 1 equiv.) (**PU 2**) and sulfide-containing diol (**12**, 1 equiv.) were added to a 50 mL round-bottom Schlenk flask attached to a nitrogen inlet line. The polyaddition was performed by mechanical stirring following the indicated conditions (i) at 120°C, under an atmosphere of N_2, for 2 h, (ii) 135°C, under an atmosphere of N_2, for 4 h. The polymers were characterized without further purification.

2.2.2 Characterization

^{1}H NMR was recorded on a Bruker Avance 400 spectrometer (400 MHz). The samples were solubilized in hot DMSO-d_6, $CDCl_3$, or $CDCl_3$+HFIP. The analyses were performed at room temperature (~25°C). From ^{1}H NMR, the alcohol and carbamate conversions were monitored in the course of the reaction by considering the signals of the OH protons of the alcohols and the NH protons of the carbamates, respectively, using a previously reported methodology [23].

Size exclusion chromatography (SEC) was used to estimate the polymer number-average molar mass (M_n), weight average molecular weight (M_w), and dispersity (Đ). Analysis were performed using HFIP as eluent on an Ultimate 3000 system from Thermoscientific equipped with a diode array detector (DAD), a multi-angle laser light scattering detector (MALS) and a differential refractive index detector (dRI) from Wyatt, using two Shodex Asahipack gel column GF310 and GF510 (300 × 7.5 mm, separation between 500 and 300 000 Da) at 50°C at a flow rate of 0.5 mL/min. The instrument was calibrated with poly(methyl methacrylate) standards.

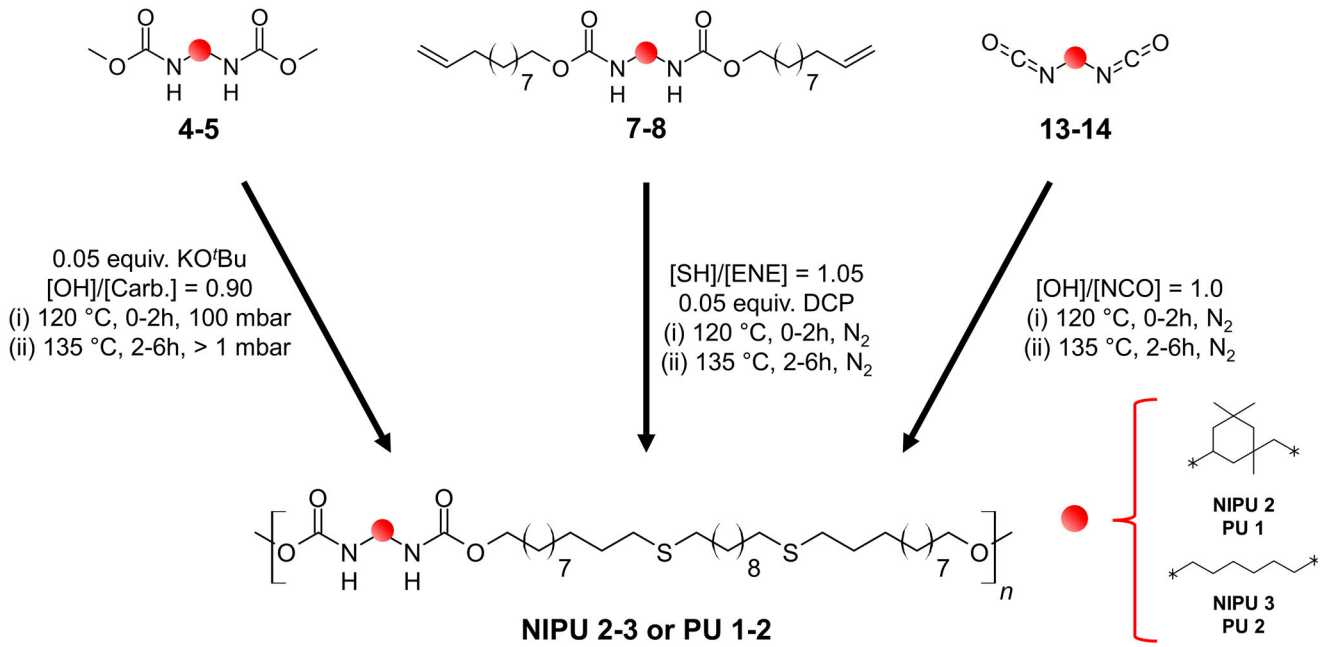

SCHEME 3 | Synthesis of poly(sulfide urethane)s via thermally initiated thiol-ene reaction of α,ω-diene carbamates in the presence of dithiols, transurethanization of dimethyl carbamates, and isocyanate polyaddition.

Polymers were analyzed by Fourier-transform infrared spectroscopy (FTIR) on a Bruker VERTEX 70 instrument on attenuated total reflectance (ATR) equipped with a DLaTGS MIR detector. The analysis was performed with a resolution of 4 cm^{-1} and 32 scans. The quantification of the urea, urethane and carbonate were calculated based on the methodology proposed by Zhang, et al. [25] and is displayed in the Supporting Information.

The polymer thermal transitions were identified by differential scanning calorimetry (DSC) using a DSC Q2000 from TA. Samples of ~ 6 mg were analyzed using a standard aluminum crucible, three temperature ramps at a heating/cooling rate of 10°C/min were applied: the first from −100 to 150°C, the second from 150 to −100°C, and the last from −100°C to 200°C.

The thermal stability of the PUs was investigated by thermogravimetry analysis (TGA). The analysis was performed on a TGA Q500 from TA Instruments. Samples of ~6 mg were heated from 30°C to 700°C at a heating rate of 10°C/min under a nitrogen atmosphere.

For the mechanical testing, NIPU films were prepared using a thermal press set to temperatures between 100°C and 135°C, depending on the specific melting temperature of the polymer. The pressing process lasted for 10 min under a pressure of approximately 6 bar. Afterward, the samples were cut into a dogbone shape with dimensions of about 3.95 mm in width and 2.08 mm in thickness. The tensile strength test was conducted on a Zwick automated testing machine, utilizing a testing speed of 20 mm/min and a preload force of 0.1 MPa.

Solid hot-melt adhesive or reactive hot-melt specimens were produced with dimensions of approximately 25 mm × 12.5 mm × 1.5 mm. For the hot-melt adhesive, the bonded joint between aluminum-NIPU-aluminum was formed using a thermal press at temperatures 120°C for 10 min, under a pressure of approximately 5 bar. For the thermally activated adhesive, the unreacted monomer mixture was poured onto the substrate fixed by a clamp. The adhesive was reacted at 135°C for 24 h. Prior to use, the aluminum substrates were cleaned with isopropanol, followed by a sandblasting treatment to eliminate any oxide layers before the bonding. The lap shear strength test was performed on a Zwick 100 machine, using a load of 2 kN and a pulling rate of 10 mm/min.

Contact angles for water and diiodomethane were measured with a Krüss MSA One-Click Surface Free Energy (SFE) system, in which approximately 2 µL of liquid was placed on the substrate or NIPUs. The total surface free energy (ν), along with its dispersive (ν^d) and polar (ν^p) components, was calculated using the Krüss Advance software.

3 Results and Discussion

3.1 Synthesis of Polyurethane by Different Pathways

In this study, dimethyl carbamates were synthesized via the methoxycarbonylation of two diamines, 1,6-hexanediamine (**2**) and isophorone diamine (**3**), in the presence of dimethyl carbonate (**1**), affording an aliphatic dimethyl carbamate (**4**) and a cycloaliphatic dimethyl carbamate (**5**), respectively. These intermediates were subsequently reacted with 10-undecen-1-ol (**6**), a renewable fatty alcohol derived from castor oil, through a transurethanization reaction to yield α,ω-diene biscarbamate monomers (**7** and **8**), as displayed in Scheme 1. The resulting monomers were fully characterized using nuclear magnetic resonance (NMR), Fourier-transform infrared spectroscopy (FTIR), size-exclusion chromatography (SEC), and differential scanning calorimetry (DSC). The analytic data are provided in Figures S1–S14.

^{1}H and ^{13}C NMR spectroscopy confirmed the formation of the targeted carbamates, no detectable side products were observed within the sensitivity limits of these techniques. However, a more detailed analysis of the FTIR spectra, based on peak deconvolution of the carbonyl stretching region (Figures S8 and S13 for compounds **7** and **8**, respectively), revealed the presence of trace amounts of urea and carbonate species. These impurities are attributed to a well-documented side reaction occurring during transurethanization, namely carbamate metathesis [23]. Based on the accepted mechanism of this reaction, the most probable side products are urea- and carbonate-containing α,ω-dienes (Scheme S1). Consistent with this interpretation, SEC analysis of both compounds displays a bimodal elution profile, characterized by a minor high–elution-time peak in addition to the main peak, which can be tentatively assigned to urea-containing α,ω-diene species. Importantly, as these side products retain an α,ω-diene structure, they are not expected to interfere with the thiol-ene polyaddition process. Their incorporation into the growing polymer chains during propagation provides an explanation for the subsequent detection of both urea and carbonate moieties within the corresponding polymers.

The resulting α,ω-diene biscarbamates were further reacted with dithiols via thiol-ene reaction, forming non-isocyanate poly(sulfide urethane)s. In this work, a thermally initiated thiol-ene approach was employed by reacting **7** with **9** in the presence of dicumyl peroxide (DCP) as the thermal initiator, as displayed in Scheme 2. The reaction was carried out in bulk using different thiol:ene molar ratios ([SH]/[Ene] = 0.8-1.2). The mixture was stirred with an overhead stirrer at 150 rpm under a constant nitrogen flow. The thermal protocol consisted of heating at 120°C for 2 hours, followed by a gradual increase to 135°C for an additional 4 hours, yielding **NIPUs 1a-g**.

The reaction progress of the different NIPU syntheses was investigated by ^{1}H NMR spectroscopy in $CDCl_3$+HFIP. The ^{1}H NMR of **NIPU 1a** is displayed in Figure 1, along with its monomer mixture before the addition of the initiator. At t = 0, partial conversion of the vinylic protons was already observed, likely due to self-initiation at relative high temperature (120°C) [26, 27]. As a result, the integration values for the vinylic CH_2 (**a**, 4.87 ppm) and CH group (**b**, 5.73 ppm) signals were 2.48 H and 1.20 protons, i.e. lower than the expected 4H and 2H, respectively. This corresponds to an estimated ene conversion of about 38% (detailed procedure for the calculation of the ene conversion is available in the ESI along with the ^{1}H NMR spectrum of **NIPU 1d**, Figure S21). In parallel, signals associated with α-sulfide protons (**a′**, 2.47 ppm) were detected, with an estimated yield of 32%, in good agreement with the observed ene conversion.

After 6 h of reaction, the ene conversion reached approximately 94% (as displayed in Table S1), while the corresponding α-sulfide proton signals accounted for about 81%, indicating that a fraction of the ene groups did not result in the expected thiol-ene coupling product. This discrepancy can be attributed to side reactions commonly associated with thiol-ene polymerizations. As reported previously, thiyl radicals may form disulfides, while ene radicals may generate branched structures [28–30]. Both pathways consume reactive species, thereby limiting the extent of the desired α-sulfide formation and reducing the overall efficiency of the reaction. Supporting this, an additional signal was observed at about 2.88 ppm by ^{1}H NMR (labeled a'' in Figure 1), which is assigned to α-protons of disulfide or chain-transfer-derived sulfide moieties. The relative integration of this peak corresponds to approximately 5 mol% of side products, reinforcing the conclusion that radical recombination processes contribute significantly to the observed discrepancy from the ideal product yield.

Due to the limited conversion and side-product formation in the thermally initiated reaction, the reaction was optimized. It is reported that adjustment of the [SH]/[Ene] ratio is fundamental to achieve high molar mass polymers following the thiol-ene methodology [30]. Fundamentally, it is expected that the maximum conversions and molar ratios are achieved in stoichiometric ratios ([SH]/[Ene] = 1.0) [29, 31].

In this context, [SH]/[Ene] ratios varying from 0.8 to 1.2 were investigated. This range was selected based on previous reports, in which the conversion, selectivity, and molar mass were controlled by varying the monomer ratio [30]. All the NIPUs were characterized using size exclusion chromatography (SEC, Figure S26) and NMR. The corresponding NIPU molar mass and the ene conversions are depicted in Figure 2.

As expected, the ene proton conversion increased proportionally with the increase of the [SH]/[Ene] ratio, in which an excess of SH promoted the highest conversion (98.1%, Table S1) for **NIPU 1 g** ([SH]/[Ene] = 1.2). Such an effect of the thiol excess on ene conversion was already observed previously [29, 30]. Despite the ene conversion increase with the [SH]/[Ene] ratio, the molar mass did not follow the same trend. Notably, the maximum M_n value (16.4 kg×mol^{-1}) was achieved for **NIPU 1e** with a slight excess of dithiol, i.e., [SH]/[Ene] = 1.05. For [SH]/[Ene] ratios higher than > 1.05, the molar mass decreased, reaching a minimum of 9.3 kg×mol^{-1} for **NIPU 1 g**. The decrease in the molar mass with a high excess of thiol was also observed elsewhere, leading to thiol-capped oligomers [32].

It is worth mentioning that **NIPUs 1b**-**1c**, obtained with an excess of ene groups ([SH]/[Ene] = 0.8 and 0.9, respectively), were partially insoluble in the $CDCl_3$+HFIP solvent mixture, making it impossible to calculate the conversion. The insolubility of these samples may arise from the formation of crosslinked structures resulting from radical-radical coupling side reactions of excess ene functionalities [30]. To demonstrate that such coupling reactions can occur under the polymerization conditions and lead to network formation, a dedicated model experiment was carried out. Specifically, the α,ω-diene isophorone-based carbamate (**8**) was heated (e.g., 135°C) in the presence of dicumyl peroxide, but in the absence of thiol. Under these conditions, the formation of an insoluble gel was observed within approximately one hour. Given that no reactive functionalities other than ene groups are present in this system, the only plausible mechanism accounting for gel formation is a radical-initiated reaction of the ene functionalities, namely radical coupling. This interpretation was further supported by exploratory rheological measurements. Time-sweep experiments performed in oscillatory mode (angular frequency = 1 rad s^{-1}, strain = 1%) showed a crossover between the storage (G′) and loss (G″) moduli at approximately 1 h, which is characteristic of gelation and confirms the formation of a crosslinked structure. Related to these observations, Burel

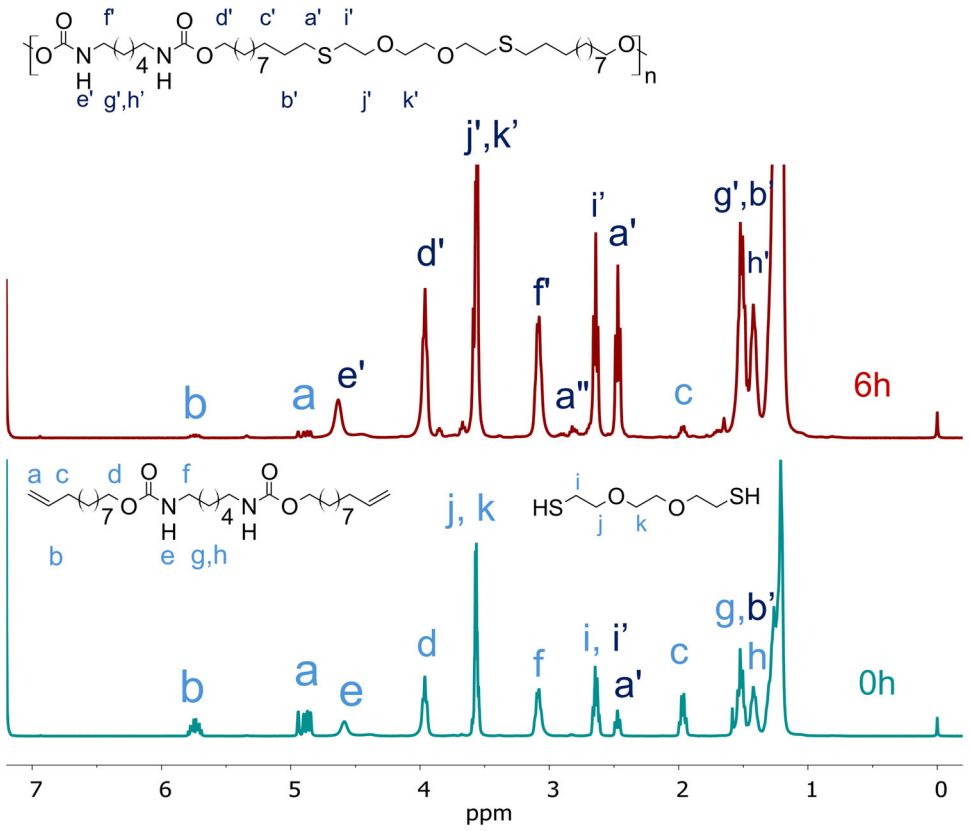

FIGURE 1 | ^{1}H NMR monitoring for the thermoinitiated thiol-ene of di(undec-10-en-1-yl) hexane-1,6-diyldicarbamate (**7**) with 1,8-dimercapto-3,6-dioxaoctane (**9**), i.e. the synthesis of **NIPU 1a** (in bulk, T = 120°C–135°C, [SH]/[Ene] = 1.0., 0.05 equiv. DCP). Top: after 6 h reaction time; bottom: monomer mixture before addition of DCP.

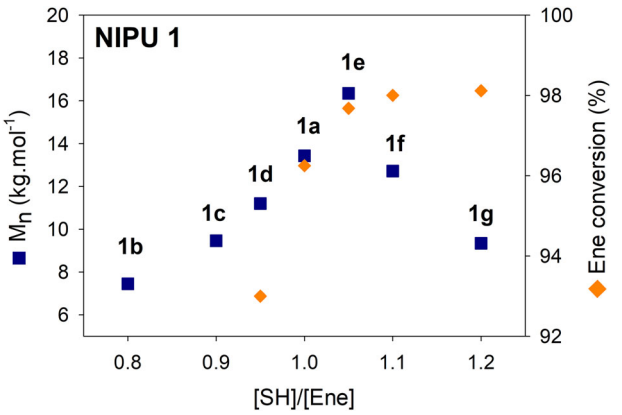

FIGURE 2 | Variation of the molecular weight, M_n, and ene conversion as a function of the thiol to ene ratio, [SH]/[Ene], for the synthesis of **NIPU 1** (bulk, 0.05 equiv. DCP). M_n was measured by SEC in HFIP and ene conversion was calculated from ^{1}H NMR in $CDCl_3$+HFIP.

et al. [22]. noticed the crosslinking of α,ω-diene non-isocyanate polyurethanes and polyureas in the presence of benzophenone as a photoinitiator, but the authors managed to achieve an ene group conversion of up to 91%.

After these initial optimizations, poly(sulfide urethane)s were synthesized via three distinct methodologies: transurethanization polycondensation, thiol-ene addition, and isocyanate-based polyaddition. To compare the synthesis methods, the same thermal protocol was applied, i.e., 120 °C for 2 h, followed by 135 °C for 4 h. In the case of the transurethanization route, a controlled vacuum was applied to efficiently remove the condensation byproducts, as illustrated in Scheme 3.

All polymers were characterized by ^{1}H NMR spectroscopy (Figures S23–S25) and SEC chromatography. Notably, NIPU 3b could not be solubilized for NMR analysis. The efficiency of the different polymerization technics was assessed by considering the molar mass characteristics obtained in SEC, as shown in Figure 3.

Among the isophorone-based poly(sulfide urethane)s, **NIPU 2a** (thiol-ene) and **NIPU 2b** (polycondensation) exhibited comparable molar mass (M_n ~20 kg×mol^{-1}, Table S1) and dispersities (Đ ~ 2). These values are higher compared to those of **PU 1** (M_n = 13.3 kg×mol^{-1}, Đ = 1.83), synthesized via isocyanate polyaddition. A similar trend was observed for the aliphatic **NIPU 1** and **NIPU 3** series (as displayed in Figure S27), indicating that non-isocyanate strategies may offer at least comparative, maybe improved, step-growth characteristics under the same reaction conditions.

As previously reported, the formation of side products, particularly urea and carbonate groups during the transurethanization of bismethylcarbamates, poses a significant limitation to this synthetic route [25]. Indeed, the incorporation of urea moieties can disrupt hydrogen bonding networks, ultimately

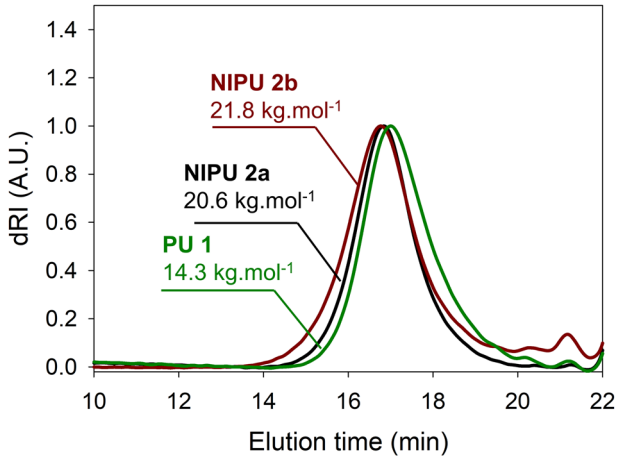

FIGURE 3 | SEC chromatograms in hexafluoroisopropanol (HFIP) of isophorone based NIPUs prepared using three different synthesis strategies (compare Scheme 3) using PMMA as a standard.

compromising the thermal and mechanical properties of the resulting polyurethanes [25]. Thus, thiol-ene polyaddition presents a promising alternative for the synthesis of non-isocyanate polyurethanes (NIPUs), as it is not expected to produce urea byproducts. To validate this hypothesis, Fourier-transform infrared (FTIR) spectroscopy was employed.

FTIR spectra of **NIPUs 2a** and **2b**, synthesized via thiol-ene and polycondensation, respectively, and **PU 1** (isocyanate-based), are shown in Figure 4a (additional spectra are provided in the supporting information, Figure S28–S30). The spectra of these materials are largely superimposable, consistent with similar backbone structures. Absorption bands characteristic of poly(sulfide urethane)s were observed, including the NH stretching vibration (~3325 cm^{-1}), NH bending (~1523 cm^{-1}) and C—S stretching (1103 cm^{-1}) [33, 34]. The carbonyl stretching region between 1740–1630 cm^{-1} further confirmed the presence of urethane linkages. Notably, **NIPU 2a** exhibited an additional weak absorption at 1637 cm^{-1}, corresponding to C=C stretching from residual alkene groups.

Due to significant peak overlap in the carbonyl region, particularly between urethane, urea, carbonate, and ene groups, spectral deconvolution was conducted to estimate individual contributions (details in ESI, Figures S28, S30). The deconvoluted peaks and relative carbonyl group contents are summarized in Table S2. Figure 4b exemplarily illustrates the deconvolution for **NIPUs 2a**.

For **NIPU 2b** (Figure S29a), seven distinct carbonyl contributions were identified: carbonate (~1740 cm^{-1}), free urethane (~1724 cm^{-1}), disordered H-bonded urethane (~1699 cm^{-1}), ordered H-bonded urethane (~1682 cm^{-1}), free urea (~1670 cm^{-1}), disordered H-bonded urea (~1660 cm^{-1}), and ordered H-bonded urea (~1630 cm^{-1}). In contrast, **PU 1** (Figure S29b) contained only urethane and urea functionalities, consistent with its synthesis via isocyanates. The presence of urea in **PU 1** likely results from partial hydrolysis of isocyanate groups due to trace water contamination [23].

For **NIPU 2a**, synthesized via thiol-ene coupling, minor signals corresponding to carbonate (1.33%) and urea groups (3.0%) were detected (Figure 4b). The presence of urea and carbonate in this sample is attributed to the carbamate metathesis side reaction that likely occurred during the synthesis of α,ω-diene carbamate via transurethanization involving the isophorone-based carbamate (**5**) and 10-undecen-1-ol (**6**) (Scheme S1).

It is noteworthy that the total urea content in **NIPU 2a** remains significantly lower than that measured for **NIPU 2b** (13.3%) and **PU 1** (8.9%) (Figure 5a, Table S2). This difference can be rationalized by considering the stage at which urea functionalities were formed. In the case of **NIPU 2a**, urea groups originated exclusively from the synthesis of the α,ω-diene monomer (**8**), as discussed above. This step is conducted under milder conditions (2 h at 90°C followed by 2 h at 120°C), thereby limiting the extent of the side reaction.

By contrast, for **NIPU 2b**, carbonate metathesis takes place during the polymerization step itself, which is performed under significantly harsher conditions (2 h at 120°C followed by 4 h at 135°C). As a consequence, the extent of the side reaction is substantially increased, resulting in a higher incorporation of urea moieties into the polymer backbone. Overall, these results highlight the thiol-ene strategy as an efficient approach to minimize the introduction of urea and carbonate functionalities in the final polymers.

However, despite its lower relative urea content, **NIPU 2a** shows a higher relative content of free urethane groups (17.6%) compared to **NIPU 2b** (14.4%) and **PU 1** (9.9%) (Figure 5b, Table S2). This increase might be due to structural irregularities introduced by branched structures generated during the radical-mediated thiol-ene process. These irregularities render the polymer chain packing more difficult and disrupt the hydrogen bonding ordering on the carbamate groups. In contrast, the higher urea content in **NIPU 2b** likely causes a statistical disruption of hydrogen-bonded domains, leading to an increase in free urethane groups [25, 35]. Similar trends regarding the relationship between synthetic route, urea content, and hydrogen bonding behavior were also observed between the **NIPU 3a-b** and **PU 2** (Figure 5; Figure S30, Table S2).

In summary, contrary to previous investigations, thermally initiated, solvent-free thiol-ene polyaddition presents a viable alternative for PU synthesis compared to conventional polyaddition polymerization, operating at relatively low temperatures (T = 90–135°C) using dicumyl peroxide as a thermal initiator and a slight excess of thiol ([SH]/[Ene] = 1.05). Polymers with relatively high molar masses (M_n up to 21 kg×mol^{-1}) can be obtained, exceeding those achieved herein via isocyanate polyaddition and polycondensation using the same temperature protocols, and with reduced urea generation. This approach outperforms most reported AIBN-initiated thermal thiol-ene reactions [5, 30] and even some photo-initiated systems. For example, Xie, et al. [16] reported NIPUs synthesized through a DMPA photo-initiated thiol-ene reaction of diene carbamates, achieving a maximum molar mass of 10 kg×mol^{-1}.

Despite the advantages in molar mass and urea suppression, NIPUs prepared via thiol-ene coupling exhibited lower hydrogen

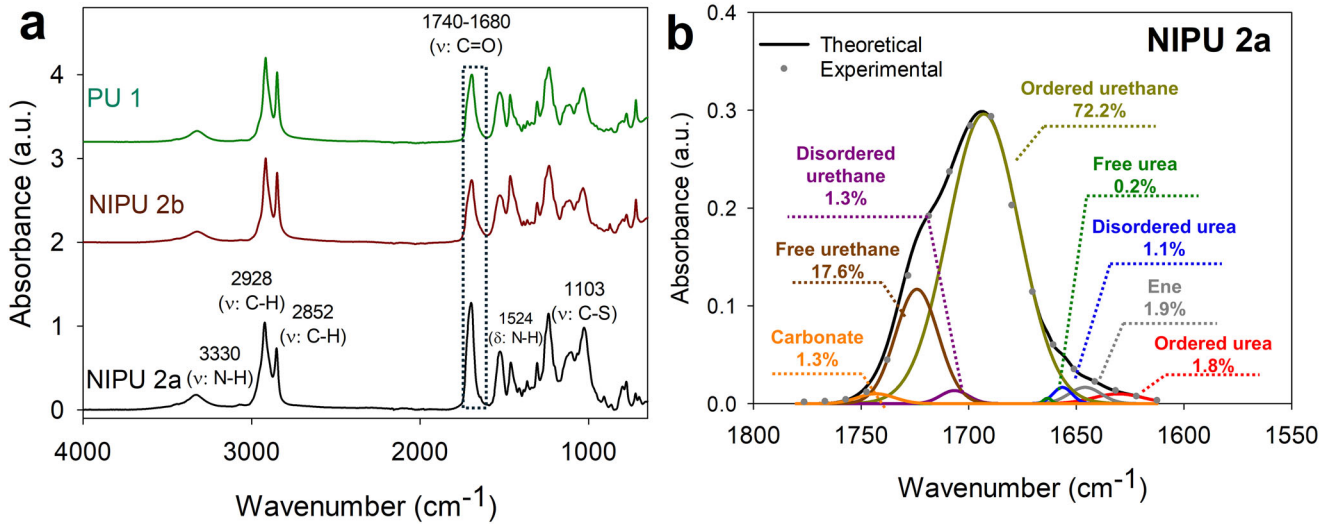

FIGURE 4 | (a) FTIR spectra of **NIPUs 2a-b** and **PU 1** with (b) peak deconvolution of the carbonyl stretching region for **NIPU 2a**.

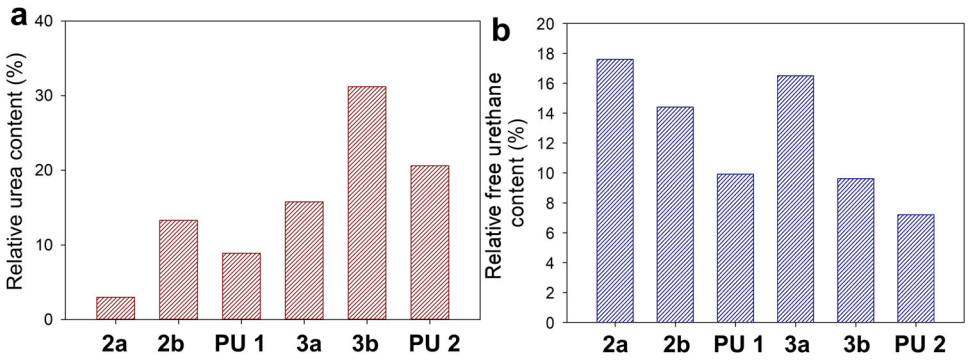

FIGURE 5 | (a) Relative urea content, and (b) relative free urethane content of **NIPUs** and **PUs** obtained by FTIR peak deconvolution.

bonding, likely due to branching and structural irregularities introduced by side reactions. This reduced order in the polymer chains disrupts microstructure formation and may impact both thermal and mechanical performance. To further assess the potential of the thermally initiated thiol-ene reaction with dicumyl peroxide, the thermal, mechanical, and adhesive properties of these NIPUs were compared with those of conventional polyurethanes synthesized from either diisocyanates or bismethyl carbamates.

3.2 Thermal and Mechanical Characterization

The thermal properties of the NIPUs (**NIPU 1–3**) and **PU 1–2** were investigated using differential scanning calorimetry (DSC) and thermogravimetric analysis (TGA). The DSC curves from the cooling and second heating ramp are presented in Figures S31–S33, while the extracted thermal parameters are summarized in Table 1.

Multiple thermal transitions were observed for the investigated NIPUs and PUs. **NIPU 3** (Figure S31) made from aliphatic carbamates, showed significantly complex thermal transitions with a T_g (~23°C), and the presence of a broad crystallization peak (T_c) centered at ~102°C and a multi-peak melting phenomenon (T_m) extending up to 127°C. Notably, a cold crystallization event was observed between melting peaks. This behavior indicates the presence of multiple crystalline domains and heterogeneous crystalline populations, consistent with previously reported behavior in poly(sulfide urethane)s [16, 36]. Although such characteristics have been reported, prior studies did not provide an explanation for this polymorphism. Similar behavior was observed for the **NIPUs 2** (Figure S31).

The influence of the three different synthesis pathways on the melting and crystallization behavior was investigated. Specifically, **NIPU 3a**, prepared via thiol-ene coupling, displayed a similar T_m of ~125 °C, however, a lower melting enthalpy (ΔH_m = 57 J/g), compared to **NIPU 3b** (ΔH_m = 85 J/g) synthesized via transurethanization and the reference polyurethane **PU 2** (ΔH_m = 81 J/g). These findings support the hypothesis that side reactions inherent to the thiol-ene process introduce branching or structural irregularities that hinder crystallinity, impacting the thermal properties of the final NIPUs. A similar trend was observed for **NIPU 2a**, compared to **NIPU 2b** and **PU 1**.

Figure 6 and Figure S34 shows the TGA and DTG curves of the different non-isocyanate polyurethanes (NIPUs) and conventional polyurethanes (PUs). The thermal parameters extracted from the thermograms are summarized in Table 1 and Table S3. Using

TABLE 1 | NIPUs thermal parameters extracted from DSC curves.

NIPUs/PU	T_g [a] (°C)	T_m [a] (°C)	ΔH_m [b] (J/g)	T_c [a] (°C)	ΔH_c [b] (J/g)	$T_{d5\%}$ (°C)
NIPU 2a	0	47	42.6[d]	—	—	289
NIPU 2b	−7	54	33.6	2/18/29[c]	14.9/14.6[c]	283
PU 1	24	98/125	81	97	78.6	334
NIPU3a	−11	89/118/127	57.4	87/93/98[c]	62/3[c]	319
NIPU 3b	23	106/117/126	85.7	85/99	75	306
PU 2	−1	53	27.5	26	27.4	328

[a]T_g, $T_{m,}$ and T_c are the glass transition, melting, and crystallization temperatures.
[b]ΔH_m and ΔH_c are the melting enthalpy and crystallization enthalpy, respectively.
[c]cold crystallization collected from the second heating.
[d]collected from the first heating ramp.

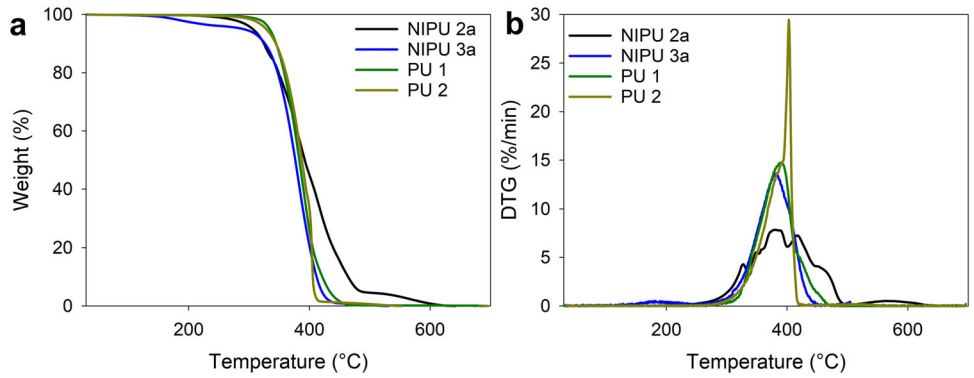

FIGURE 6 | (a) TGA and (b) DTG curves of poly(sulfide urethane)s.

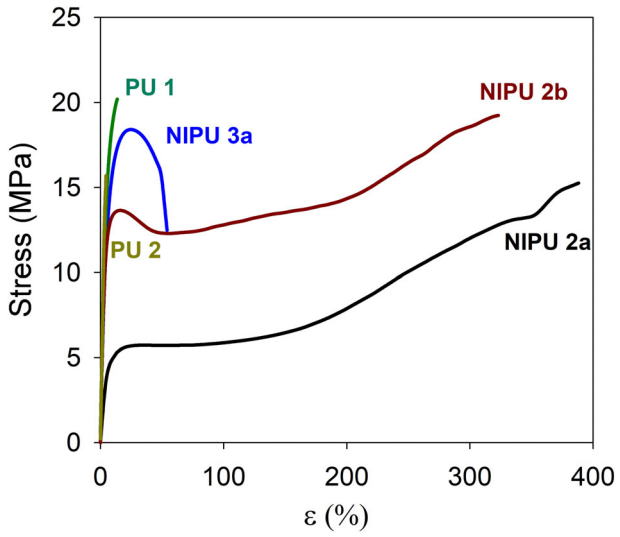

FIGURE 7 | Stress-strain curves for the different NIPUs and PUs.

the temperature at 5% weight loss ($T_{d5\%}$) to compare thermal stability, the NIPUs exhibited degradation temperatures ranging from 266 to 344°C. The variation in thermal stability is attributed to differences in chemical structure, including the number of urethane linkages, the presence of sulfur atoms, and the carbon chain length and rigidity of the incorporated monomers [3, 37, 38].

In terms of polymerization method, NIPUs prepared via polycondensation and those synthesized through thiol-ene polyaddition exhibited comparable thermal stabilities. However, both conventional PUs (**PU 1** and **PU 2**) showed significantly higher $T_{d5\%}$ values than their NIPU counterparts (**NIPU 2** and **3**, respectively). For instance, isophorone-based **NIPU 2** presented a $T_{d5\%}$ of approximately 285°C, while **PU 1** exhibited a value of 328°C. This difference is likely due to residual components from the synthesis process. In the case of NIPUs prepared by thiol–ene polyaddition, traces of radical initiator fragments (e.g., peroxides), and for those synthesized via transurethanization, residual metal alkoxide catalysts, may remain in the polymer [39–41]. These species can catalyze degradation reactions by initiating polymer pyrolysis [39, 40], or by the introduction of weak bonds to the polymer structure [41]. This problem can be circumvented by further polymer purification [39, 40]. While further purification could mitigate this issue, such processes are challenging due to the limited solubility of poly(sulfide urethane)s (mostly soluble in toxic HFIP), making conventional purification routes, such as precipitation, impractical.

The mechanical properties of the NIPUs and PUs were evaluated through tensile tests. Polymer films with a thickness of approximately 1.3 mm were prepared by hot pressing at 120°C and 4 bar pressure for about 10 min. The films were then shaped using a dogbone die attached to a toggle press and subjected to tensile testing. A representative stress-strain curves is provided for each NIPUs and PUs in Figure 7. Measurements were performed

TABLE 2 | Mechanical properties of the different NIPUs and PUs.

	Young's Modulus (MPa)[a]	Tensile strength (MPa)[a]	Elongation at break (%)[a]
NIPU 2a	140.0 ± 10.3	13.0 ± 2.00	342.7 ± 43.4
NIPU 2b	415.7 ± 2.4	17.3 ± 0.5	304.7 ± 26.0
PU 1	462.0 ± 37.8	15.0 ± 1.2	9.0 ± 3.7
NIPU 3a	370.8 ± 0.1	10.9 ± 0.9	70.2 ± 20.1
PU 2	457.8 ± 33.0	14.7 ± 0.8	6.9 ± 0.2

[a]Estimated by tensile strength test with a constant deformation of 20 mm/min.

in triplicate (Figures S35–S36), and the corresponding data are summarized in Table 2.

The Young's moduli for the analyzed NIPUs ranged from 140 to 460 MPa, with the tensile strength at break between 13 and 43 MPa, and elongation at break varying from 10% to 350%. The polymers exhibited a range of mechanical behaviors, from brittle to ductile, with some samples showing a yield point and strain-induced crystallization [42, 43]. The observed mechanical properties are primarily influenced by the rigidity of the poly(sulfide urethane) structures, which are controlled by factors such as the polymerization method, hydrogen bonding, and crystallization characteristics [44].

The polymerization method significantly influenced the mechanical properties of the isophorone-based polyurethanes, particularly in **NIPUs 2a**, **2b**, and **PU 1**. **NIPU 2a**, synthesized via thiol-ene polyaddition, exhibited lower tensile strength (13 MPa) and a reduced Young's Modulus (140 MPa) compared to **NIPU 2b** (17.3 and 415,7 MPa, respectively). This behavior can be attributed to two factors: (i) a lower density of hydrogen bonding in **NIPU 2a**, as discussed above, and (ii) a less crystalline morphology, likely resulting from the thermal treatment (120°C for 10 min) applied during dogbone sample preparation. As hypothesized during the DSC analysis, this processing step may have reduced the degree of crystallinity, thereby increasing chain mobility and reducing stiffness [45–47].

A comparison between **NIPU 2b** (transurethanization) and **PU 1**, both prepared using the same sulfide diol (**11**) and exhibiting similar crystallization behavior, was also analyzed. **PU 1** showed a slightly higher Young's Modulus (462 MPa) but significantly lower elongation at break (9%) than **NIPU 2b** (304%). This difference is primarily attributed to the higher urea content in **NIPU 2b**. While urea linkages generally contribute to increased rigidity, their statistical distribution in **NIPU 2b** reduces hydrogen bonding efficiency within crystalline regions, thus enhancing flexibility. On the other hand, **PU 1** contains fewer urea groups and exhibits higher hydrogen bonding interactions, resulting in a stiffer, less flexible polymer. These results highlight the combined influence of polymerization route, urea content, and hydrogen bonding on the mechanical properties of the resulting polyurethanes. Similar behavior was observed between the linear aliphatic-based carbamates **NIPU 3a** and **PU 2**.

Lap shear tests were conducted on samples derived from isophorone-based polyurethanes, chosen for their lower melting points and improved processability. For thermoplastic hot melt adhesives prepared by different synthesis methods, specifically **NIPUs 2a** (thiol-ene), **2b** (transurethanization), and **PU 1**, bonding was achieved using a hot-melt technique. Films measuring 1.3 mm × 25 mm were placed between aluminum substrates and bonded using a thermopress at 120°C for 10 min under a pressure of 5 bar. A typical lap shear stress–displacement curves is provided for **NIPUs 2** and **PU 1** in Figure 8. Measurements were performed in triplicate (Figure S37), and the corresponding data are summarized in Table S4.

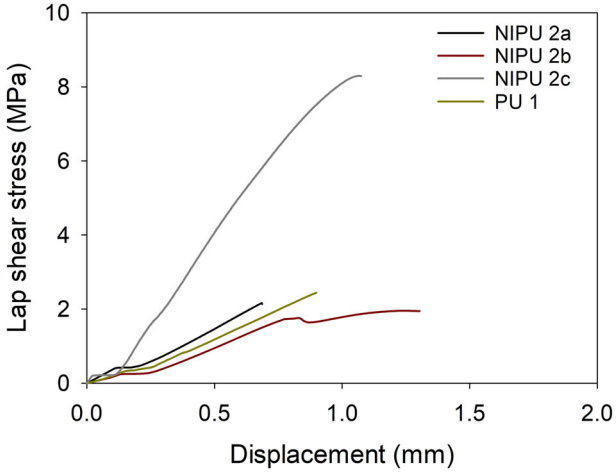

FIGURE 8 | Lap shear stress-displacement curves for the different aluminum-NIPU-aluminum joints.

NIPUs 2 and **PU 1** achieved a relatively low lap shear strength value of ~2.1 MPa with adhesive failure modes. This indicates that, for thermoplastic hot-melt adhesives, the synthetic method itself does not significantly impact adhesive strength. Despite differences in polarity between **NIPU 2** and **PU 1**, as indicated by contact angle measurements with water and diiodomethane (Figures S38–S40), both materials present surface free energy (γ^s) values exceeding that of aluminum (Figure S38b), suggesting poor wettability with the substrate [48]. As a result, insufficient interfacial contact may be limiting good adhesion performance. In such cases, wettability can be improved by increasing bonding temperature or time, which lowers polymer viscosity and enhances substrate wetting [49, 50].

Inspired by these observations, the thiol-ene polymerization was performed directly on the substrate. To this end, a liquid formulation consisting of the isophorone-based α,ω-diene (**8**, 1 equiv.), 1,10-decanedithiol (**10**, 1.05 equiv.), and **DCP** (0.05 equiv.),

i.e. identical to that used for the synthesis of **NIPU 2a**, was sandwiched between two aluminum plates held in place with clamps. The assembly was heated at 135°C for 24 h to initiate and sustain the thiol-ene polymerization, yielding an adhesive material hereafter referred to as **NIPU 2c**. Compared to **NIPU 2a**, **NIPU 2c** is subjected to a substantially longer exposure to elevated temperature. Indeed, **NIPU 2a** was synthesized in bulk using a two-step thermal program (120°C for 2 h followed by 135°C for 4 h) and subsequently applied as an adhesive by a hot-melt process at 120°C for 10 min under a pressure of 5 bar. In contrast, the in situ polymerization used to generate **NIPU 2c** proceeds entirely under adhesive-forming conditions at 135°C. As a result, **NIPU 2c** showed a marked improvement in lap-shear performance, characterized by cohesive failure (Figure S41) and an adhesion strength of 8.1 MPa, which is nearly four times higher than that measured for NIPU 2a (2.1 MPa). These results indicate that direct thiol-ene polymerization on aluminum substrates under prolonged high-temperature conditions significantly enhances adhesive performance. This improvement is likely associated with superior initial substrate wettability afforded by liquid deposition, as well as enhanced polymer chain mobility and interfacial wetting resulting from extended curing times at elevated temperature. Together, these factors promote improved cohesive properties and stronger interfacial contact between the adhesive and the substrate. Finally, it cannot be excluded that the prolonged thermal exposure experienced by **NIPU 2c** may induce additional side reactions or partial crosslinking, which could further contribute to the observed enhancement in adhesion properties.

These results highlight the potential of thermally-initiated thiol-ene coupling as a greener and safer alternative for the development of high-performance polyurethane adhesives.

4 Conclusion

This study presents a comparative analysis of three synthetic strategies, thermally initiated thiol-ene polyaddition, isocyanate-based polyaddition, and transurethanization, for the development of poly(sulfide urethane)s. Among these, the thiol-ene approach emerged as a particularly promising route.

By employing a thermally initiated radical mechanism using dicumyl peroxide as the initiator and a slight stoichiometric excess of thiol functional groups ([SH]/[Ene] = 1.05), the thiol–ene route enabled the synthesis of high-molar-mass NIPUs with expected dispersity ($Đ \sim 2$). The molar masses achieved via thiol-ene polymerization were superior to those obtained through both isocyanate-based and polycondensation routes under equivalent processing conditions. Notably, this method also minimized the formation of undesirable urea and carbonate moieties.

The thermal and mechanical properties of the NIPUs were assessed through TGA, DSC, and tensile testing. The materials exhibited degradation temperatures above 270°C and displayed semicrystalline behavior, with melting transitions ranging from 50°C to 130°C. Thiol-ene derived NIPUs demonstrated comparable thermal transitions and tensile strength to conventional polyurethanes, while also achieving higher elongation at break and moderate Young's moduli, highlighting the mechanical tunability of the materials.

Adhesive strength was also enhanced on aluminum as a substrate, likely due to stronger interfacial interactions attributed to the capability of sulfur to generate hydrogen bonding. In addition, the use of a thermally activated reactive bonding strategy, where polymerization occurred directly at the interface, led to a substantial improvement in adhesive performance. Under these conditions, lap shear strength increased by more than threefold relative to conventional hot-melt application, with cohesive failure observed across bonded joints.

Overall, these findings demonstrate the potential of thiol-ene polyaddition as a safer, isocyanate-free route to high-performance polyurethanes with enhanced thermal resistance and adhesive strength. The combination of structural tunability, efficient polymerization, and favorable application properties makes this strategy highly promising for next-generation coating and adhesive systems.

Acknowledgements

The authors would like to express thanks for the financial support provided by the NIPU-EJD project; this project has received funding from the European Union's Horizon 2020 research and innovation program under Marie Skłodowska-Curie Grant Agreement No. 955700.

Open access funding enabled and organized by Projekt DEAL.

Conflicts of Interest

The authors declare no conflicts of interest.

Data Availability Statement

The data that support the findings of this study are available in the supplementary material of this article.

References

1. M. Rogulska, "Transparent Sulfur-containing Thermoplastic Polyurethanes with Polyether and Polycarbonate Soft Segments," *Polymer Bulletin* 75 (2018): 1211–1235, https://doi.org/10.1007/s00289-017-2088-x.

2. A. Kultys, W. Podkościelny, and S. Pikus, "Polyurethanes Containing Sulfur. I. New Thermoplastic Polyurethanes with Benzophenone Unit in Their Structure," *Journal of Polymer Science Part A: Polymer Chemistry* 37 (1999): 4140–4150, https://doi.org/10.1002/(SICI)1099-0518(19991115)37.

3. S. Oprea, D. Timpu, and V. Oprea, "Design-properties Relationships of Polyurethanes Elastomers Depending on Different Chain Extenders Structures," *Journal of Polymer Research* 26 (2019): 1–15, https://doi.org/10.1007/s10965-019-1777-6.

4. X. Pan, J. Li, F. Liu, C. Hu, and Y. Zeng, "Self-Healable, Weldable, and Reprocessable Castor Oil-Based Poly(thiourethane-urethane) Networks," *Journal of Applied Polymer Science* 140 (2023): 54539, https://doi.org/10.1002/app.54539.

5. L. Filippi and M. A. Meier, "Fully Renewable Non-Isocyanate Polyurethanes via the Lossen Rearrangement," *Macromolecular Rapid Communications* 42 (2021): 2000440, https://doi.org/10.1002/marc.202000440.

6. G. Coste, D. Berne, V. Ladmiral, C. Negrell, and S. Caillol, "Non-isocyanate Polyurethane Foams Based on Six-membered Cyclic Carbon-

ates," *European Polymer Journal* 176 (2022): 111392, https://doi.org/10.1016/j.eurpolymj.2022.111392.

7. L. Maisonneuve, O. Lamarzelle, E. Rix, E. Grau, and H. Cramail, "Isocyanate-free Routes to Polyurethanes and Poly (hydroxy urethane) s," *Chemical Reviews* 115 (2015): 12407–12439, https://doi.org/10.1021/acs.chemrev.5b00355.

8. A. Llevot and M. Meier, "Perspective: Green Polyurethane Synthesis for Coating Applications," *Polymer International* 68 (2019): 826–831, https://doi.org/10.1002/pi.5655.

9. Y. Chen, B. Chen, and J. M. B. Torkelson, "Biobased, Reprocessable Non-isocyanate Polythiourethane Networks with Thionourethane and Disulfide Cross-Links: Comparison with Polyhydroxyurethane Network Analogues," *Macromolecules* 56 (2023): 3687–3702, https://doi.org/10.1021/acs.macromol.3c00220.

10. E. Vanbiervliet, S. Fouquay, G. Michaud, F. Simon, J.-F. Carpentier, and S. M. Guillaume, "Non-Isocyanate Polythiourethanes (NIPTUs) from Cyclodithiocarbonate Telechelic Polyethers," *Macromolecules* 52 (2019): 5838–5849, https://doi.org/10.1021/acs.macromol.9b00695.

11. F. Monie, B. Grignard, and C. Detrembleur, "Divergent Aminolysis Approach for Constructing Recyclable Self-Blown Nonisocyanate Polyurethane Foams," *ACS Macro Letters* 11 (2022): 236–242, https://doi.org/10.1021/acsmacrolett.1c00793.

12. M. Chaib, S. El Khezraji, S. Thakur, H. B. Youcef, M. Lahcini, and R. S. Verdejo, "Self-blowing, Hybrid Non-isocyanate Polyurethane Foams Produced at Room Temperature," *Reactive and Functional Polymers* 200 (2024): 105924, https://doi.org/10.1016/j.reactfunctpolym.2024.105924.

13. P. Helbling, F. Hermant, M. Petit, T. Vidil, and H. Cramail, "Design of Plurifunctional Cyclocarbonates and Their Use as Precursors of Poly(hydroxyurethane) Thermosets: A Review," *Macromolecular Chemistry and Physics* 224 (2023): 2300300, https://doi.org/10.1002/macp.202300300.

14. F. C. Destaso, C. Libretti, C. Le Coz, E. Grau, H. Cramail, and M. A. R. Meier, "Optimized Synthesis of a High Oleic Sunflower Oil Derived Polyamine and Its Lignin-based NIPUs," *Green Chemistry* 27 (2025): 1440–1450, https://doi.org/10.1039/D4GC05645K.

15. F. C. M. Scheelje and M. A. R. Meier, "Non-isocyanate Polyurethanes Synthesized from Terpenes Using Thiourea Organocatalysis and Thiol-ene-chemistry," *Communications Chemistry* 6 (2023): 239, https://doi.org/10.1038/s42004-023-01041-x.

16. H. Xie, S. Xie, Y. Li, Y. Chai, Q. Chen, and M. North, "Introducing the Reversible Reaction of CO2 with Diamines into Nonisocyanate Polyurethane Synthesis," *ACS Macro Letters* 13 (2024): 14–20, https://doi.org/10.1021/acsmacrolett.3c00621.

17. M. Calle, G. Lligadas, J. C. Ronda, M. Galià, and V. Cádiz, "An Efficient Nonisocyanate Route to Polyurethanes via Thiol-Ene Self-Addition," *Journal of Polymer Science Part A: Polymer Chemistry* 52 (2014): 3017–3025, https://doi.org/10.1002/pola.27347.

18. M. Shibata, N. Ishigami, and A. Shibita, "Synthesis of Sugar Alcohol-derived Water-soluble Polyamines by the Thiol-ene Reaction and Their Utilization as Hardeners of Water-soluble Bio-based Epoxy Resins," *Reactive and Functional Polymers* 118 (2017): 35–41, https://doi.org/10.1016/j.reactfunctpolym.2017.07.003.

19. O. Lamarzelle, G. Hibert, S. Lecommandoux, E. Grau, and H. Cramail, "A Thioglycerol Route to Bio-based Bis-cyclic Carbonates: Poly(hydroxyurethane) Preparation and Post-functionalization," *Polymer Chemistry* 8 (2017): 3438–3447, https://doi.org/10.1039/C7PY00556C.

20. M. Desroches, R. Auvergne, B. Boutevin, and S. Caillol, "Synthesis of Bio-based Building Blocks from Vegetable Oils: A Platform Chemicals Approach," *Oléagineux, Corps gras, Lipides* 20 (2013): 16–22, https://doi.org/10.1002/lite.201400014.

21. L. Maisonneuve, A.-L. Wirotius, C. Alfos, E. Grau, and H. Cramail, "Fatty Acid-based (bis) 6-membered Cyclic Carbonates as Efficient Isocyanate Free Poly(hydroxyurethane) Precursors," *Polymer Chemistry* 5 (2014): 6142–6147, https://doi.org/10.1039/C4PY00922C.

22. A. Martin, L. Lecamp, H. Labib, F. Aloui, N. Kébir, and F. Burel, "Synthesis and Properties of Allyl Terminated Renewable Non-isocyanate Polyurethanes (NIPUs) and Polyureas (NIPUreas) and Study of Their Photo-crosslinking," *European Polymer Journal* 84 (2016): 828–836, https://doi.org/10.1016/j.eurpolymj.2016.06.008.

23. N. G. Jaques, T. Vidil, A. Llevot, É. Grau, M. A. R. Meier, and H. Cramail, "High Molar Mass Non-Isocyanate Polyurethanes by Transurethanization of Diols with Isophorone-Based Bismethylcarbamate," *Macromolecular Chemistry and Physics* 226 (2025): 2500068, https://doi.org/10.1002/macp.202500068.

24. O. Türünç and M. A. R. Meier, "Fatty Acid Derived Monomers and Related Polymers via Thiol-ene (Click) Additions," *Macromolecular Rapid Communications* 31 (2010): 1822–1826, https://doi.org/10.1002/marc.201000291.

25. B. Zhang, Z. Shen, L. Zheng, et al., "A Comparison of Non-isocyanate and HDI-based Poly (ether urethane): Structure and Properties," *Polymer* 175 (2019): 186–194, https://doi.org/10.1016/j.polymer.2019.05.010.

26. Y. Zuo, J. Cao, and S. Feng, "Sunlight-Induced Cross-Linked Luminescent Films Based on Polysiloxanes and D -Limonene via Thiol–ene "Click" Chemistry," *Advanced Functional Materials* 25 (2015): 2754–2762, https://doi.org/10.1002/adfm.201500187.

27. U. Biermann, W. Butte, R. Koch, et al., "Initiation of Radical Chain Reactions of Thiol Compounds and Alkenes without any Added Initiator: Thiol-Catalyzed Cis/Trans Isomerization of Methyl Oleate," *Chemistry – A European Journal* 18 (2012): 8201–8207, https://doi.org/10.1002/chem.201103252.

28. İ. Degirmenci, "Role of Initiator Structure on Thiol-Ene Polymerization: a Comprehensive Theoretical Study," *Journal of the Turkish Chemical Society Section A: Chemistry* 9 (2022): 149–162, https://doi.org/10.18596/jotcsa.1003469.

29. S. P. S. Koo, M. M. Stamenović, R. A. Prasath, et al., "Limitations of Radical Thiol-Ene Reactions for Polymer–polymer Conjugation," *Journal of Polymer Science Part A: Polymer Chemistry* 48 (2010): 1699–1713, https://doi.org/10.1002/pola.23933.

30. H. Mutlu, A. N. Parvulescu, P. C. A. Bruijnincx, B. M. Weckhuysen, and M. A. R. Meier, "On the Polymerization Behavior of Telomers: Metathesis versus Thiol–Ene Chemistry," *Macromolecules* 45 (2012): 1866–1878, https://doi.org/10.1021/ma2026572.

31. C. E. Hoyle and C. N. Bowman, "Thiol–Ene Click Chemistry," *Angewandte Chemie International Edition* 49 (2010): 1540–1573, https://doi.org/10.1002/anie.200903924.

32. H. Li, S. Thanneeru, L. Jin, C. J. Guild, and J. He, "Multiblock Thermoplastic Elastomers via One-pot Thiol–ene Reaction," *Polymer Chemistry* 7 (2016): 4824–4832, https://doi.org/10.1039/C6PY00822D.

33. S. Ma, H. Zhang, R. J. Sablong, C. E. Koning, and R. A. T. M. Van Benthem, "t -Butyl-Oxycarbonylated Diamines as Building Blocks for Isocyanate-Free Polyurethane/Urea Dispersions and Coatings," *Macromolecular Rapid Communications* 39 (2018): 1800004, https://doi.org/10.1002/marc.201800004.

34. P. Deepa and M. Jayakannan, "Solvent-Free and Nonisocyanate Melt Transurethane Reaction for Aliphatic Polyurethanes and Mechanistic Aspects," *Journal of Polymer Science Part A: Polymer Chemistry* 46 (2008): 2445–2458, https://doi.org/10.1002/pola.22578.

35. E. Sarlin, S. Kotanen, T. Wirtanen, et al., "Cyclic Carbonates as Building Blocks for Non-isocyanate Polyurethanes," *Journal of Applied Polymer Science* 140 (2023): 53964, https://doi.org/10.1002/app.53964.

36. M. Rogulska, W. Podkościelny, A. Kultys, S. Pikus, and E. Poździk, "Studies on Thermoplastic Polyurethanes Based on New Diphenylethane-derivative Diols. I. Synthesis and Characterization of Nonsegmented Polyurethanes from HDI and MDI," *European Polymer Journal* 42 (2006): 1786–1797, https://doi.org/10.1016/j.eurpolymj.2006.02.014.

37. W. Lei, C. Fang, X. Zhou, Y. Cheng, R. Yang, and D. Liu, "Morphology and Thermal Properties of Polyurethane Elastomer Based on Representa-

tive Structural Chain Extenders," *Thermochimica Acta* 653 (2017): 116–125, https://doi.org/10.1016/j.tca.2017.04.008.

38. N. Kébir, M. Benoit, and F. Burel, "Elaboration of AA-BB and AB-type Non-Isocyanate Polyurethanes (NIPUs) Using a Cross Metathesis Polymerization between Methyl Carbamate and Methyl Carbonate Groups," *European Polymer Journal* 107 (2018): 155–163, https://doi.org/10.1016/j.eurpolymj.2018.07.045.

39. T. Mori, H. Nishida, Y. Shirai, and T. Endo, "Effects of Chain End Structures on Pyrolysis of Poly(-lactic acid) Containing Tin Atoms," *Polymer Degradation and Stability* 84 (2004): 243–251, https://doi.org/10.1016/j.polymdegradstab.2003.11.008.

40. Y. Fan, H. Nishida, Y. Shirai, Y. Tokiwa, and T. Endo, "Thermal Degradation Behaviour of Poly(lactic acid) Stereocomplex," *Polymer Degradation and Stability* 86 (2004): 197–208, https://doi.org/10.1016/j.polymdegradstab.2004.03.001.

41. J. Krstina, G. Moad, and D. H. Solomon, ""Weak Links" in Polystyrene—Thermal Degradation of Polymers Prepared with AIBN or Benzoyl Peroxide as Initiator," *European Polymer Journal* 25 (1989): 767–777, https://doi.org/10.1016/0014-3057(89)90043-8.

42. M. Rogulska, A. Kultys, and E. Olszewska, "New Thermoplastic Poly(thiourethane-urethane) Elastomers Based on Hexane-1,6-diyl Diisocyanate (HDI)," *Journal of Thermal Analysis and Calorimetry* 114 (2013): 903–916, https://doi.org/10.1007/s10973-013-3007-5.

43. R. S. Waletzko, L. T. J. Korley, B. D. Pate, E. L. Thomas, and P. T. Hammond, "Role of Increased Crystallinity in Deformation-Induced Structure of Segmented Thermoplastic Polyurethane Elastomers with PEO and PEO−PPO−PEO Soft Segments and HDI Hard Segments," *Macromolecules* 42 (2009): 2041–2053, https://doi.org/10.1021/ma8022052.

44. S. Torresi, T. Calvo-Correas, S. Basasoro, et al., "Furan-containing Biobased Polyurethane Nanofibers: A New Versatile and Green Support Clickable via Diels-Alder Reaction," *Reactive and Functional Polymers* 178 (2022): 105353, https://doi.org/10.1016/j.reactfunctpolym.2022.105353.

45. M. Amirkhosravi, L. Yue, T. Ju, and I. Manas-Zloczower, "Designing Thermal Annealing to Control Mechanical Performance of Thermoplastic Polyurethane Elastomers," *Polymer* 214 (2021): 123254, https://doi.org/10.1016/j.polymer.2020.123254.

46. Y. Li, T. Gao, J. Liu, K. Linliu, C. R. Desper, and B. Chu, "Multiphase Structure of a Segmented Polyurethane: Effects of Temperature and Annealing," *Macromolecules* 25 (1992): 7365–7372, https://doi.org/10.1021/ma00052a045.

47. Y. Yanagihara, N. Osaka, S. Murayama, and H. Saito, "Thermal Annealing Behavior and Structure Development of Crystalline Hard Segment Domain in a Melt-quenched Thermoplastic Polyurethane," *Polymer* 54 (2013): 2183–2189, https://doi.org/10.1016/j.polymer.2013.02.005.

48. S. Gharde, G. Sharma, and B. Kandasubramanian *Progress in Adhesion and Adhesives* (Wiley, 2021), pp. 1–28.

49. H. Wu, Y. Chen, W. Zhu, Y. Shangguan, and Q. Zheng, "Highly Adhesive and Tough Thermoplastic Polyurethanes Using a Furandicarboxamide Rigid Chain Extender with Noncovalent Interactions," *ACS Applied Polymer Materials* 5 (2023): 3515–3523, https://doi.org/10.1021/acsapm.3c00198.

50. B. Shi, X. Xu, J. Zhong, et al., "Comparison and Investigation of H-bond Assisted Reusable PU Adhesives with High Shear Strength," *Progress in Organic Coatings* 192 (2024): 108508, https://doi.org/10.1016/j.porgcoat.2024.108508.

Supporting Information

Additional supporting information can be found online in the Supporting Information section.

Supporting File: macp70196-sup-0001-SuppMat.pdf.